

Pyramid Quantile Regression

T. Rodrigues^{*†}, J.-L. Dortet-Bernadet[‡] and Y. Fan^{*§}

Abstract

Quantile regression models provide a wide picture of the conditional distributions of the response variable by capturing the effect of the covariates at different quantile levels. In most applications, the parametric form of those conditional distributions is unknown and varies across the covariate space, so fitting the given quantile levels simultaneously without relying on parametric assumptions is crucial. In this work we propose a Bayesian model for simultaneous linear quantile regression. More specifically, we propose to model the conditional distributions by using random probability measures known as quantile pyramids. Unlike many existing approaches, our framework allows us to specify meaningful priors on the conditional distributions, whilst retaining the flexibility afforded by the nonparametric error distribution formulation. Simulation studies demonstrate the flexibility of the proposed approach in estimating diverse scenarios, generally outperforming other competitive methods. We also provide conditions for posterior consistency. The method is particularly promising for modelling the extremal quantiles. Applications to extreme value analysis and in higher dimensions are also explored through real data examples.

^{*}School of Mathematics and Statistics, University of New South Wales, Sydney 2052 Australia.

[†]CAPES Foundation, Ministry of Education of Brazil, Brasília - DF 70040-020, Brazil

[‡]Institut de Recherche Mathématique Avancée, UMR 7501 CNRS, Université de Strasbourg, Strasbourg, France.

[§]Communicating Author: Y.Fan@unsw.edu.au

Keywords: Bayesian quantile pyramid; Simultaneous quantile regression; Extremal quantile regression.

1 Introduction

Since the seminal work by Koenker and Bassett (1978) linear quantile regression has been recognized in recent years as a robust statistical procedure that offers a powerful and compelling alternative to ordinary linear mean regression. It has been successfully applied to a diverse range of fields whenever interest lies in the non-central parts of the response distribution, often found in the environmental sciences, medicine, engineering and economics. Let $\tau, 0 < \tau < 1$, be a probability value and let \mathcal{X} be a bounded subspace of \mathbb{R}^P , for an integer $P \geq 1$. The linear τ -th quantile regression model specifies the conditional distribution of a real response variable Y given the value $X = \mathbf{x}$ of a P dimensional vector of covariates

$$Y|\mathbf{x} \sim \beta_\tau^0 + \mathbf{x}'\beta_\tau + \epsilon, \tag{1}$$

for some unknown coefficients $\beta_\tau^0 \in \mathbb{R}$ and $\beta_\tau \in \mathbb{R}^P$, and for a noise variable ϵ whose τ -th conditional quantile is 0, *i.e.* $Q_\epsilon(\tau|\mathbf{x}) \equiv \inf\{a : P(\epsilon \leq a|X = \mathbf{x}) \geq \tau\} = 0$ or $\mathbb{P}(\epsilon \leq 0|X = \mathbf{x}) = \tau$. Equivalently, we can write the τ -th quantile of the conditional distribution of Y given $X = \mathbf{x}$ as $Q_Y(\tau|\mathbf{x}) = \beta_\tau^0 + \mathbf{x}'\beta_\tau$.

Let $(y_i, \mathbf{x}_i)_{i=1, \dots, N}$ be N observed values of (Y, X) . Frequentist inference on the linear quantile regression model typically leaves the noise distribution unspecified and the estimation of $(\beta_\tau^0, \beta_\tau)$ is carried out by solving the minimization problem,

$$(\hat{\beta}_\tau^0, \hat{\beta}_\tau) = \arg \min_{(\beta^0, \beta)} \sum_{i=1}^N \rho_\tau(y_i - \beta^0 - \mathbf{x}_i' \beta),$$

where the so-called “check function” $\rho_\tau(\cdot)$ is given by $\rho_\tau(\epsilon) = \tau\epsilon$ if $\epsilon \geq 0$ and $\rho_\tau(\epsilon) = (\tau - 1)\epsilon$ otherwise (see Koenker and Bassett 1978). Inference is usually based on asymptotic arguments, see Koenker (2005) for more details and properties of this approach. Bayesian treatment of quantile regression is more challenging, since a specification of a likelihood can be problematic. In recent years, the asymmetric Laplace error model has emerged as a popular tool for Bayesian inference (Yu and Moyeed 2001), largely due to its flexibility and simplicity, and the fact that the corresponding maximum likelihood estimate is the solution of the minimization problem above. It was shown in Sriram et al. (2013) that, under mild conditions, the asymmetric Laplace can produce a Bayesian consistent posterior inference for the case of linear quantiles. However, in applications to real data, we do not really expect the distribution of the underlying data to follow an asymmetric Laplace distribution. Empirically, several authors have demonstrated that the asymmetric Laplace model does not have good coverage probabilities, see for exam-

ple Reich et al. (2008). Other authors have tried to model the error distribution flexibly with nonparametric distributions, constraining the τ -th quantile of the error distribution to be zero. See *e.g.* Kottas and Gelfand (2001), Hanson and Johnson (2002), Kottas and Krnjajić (2009) or Reich et al. (2008) who propose the use of various nonparametric distributions including infinite mixture of Gaussians, Dirichlet process mixtures and mixture of Pólya trees.

In many applications, quantile estimates at several different quantile levels are needed to provide a precise description of the conditional distribution. A well known problem with separately fitted quantile regression planes is that they can cross, violating the definition of quantiles. A possible solution is to use a second stage adjustment to the initial fits, see for example Hall et al. (1999), Dette and Volgushev (2008) and Chernozhukov et al. (2009) in the frequentist setting, or more recently Rodrigues and Fan (2016) in a Bayesian setting. Another possible solution is a joint estimation of multiple quantiles. This has been advocated by several authors, as it leads naturally to a greater borrowing of information across quantiles and a higher global efficiency for all quantiles of interest. Under this paradigm, Reich et al. (2011) proposed a model using Bernstein basis polynomials for spatial quantile regression. Tokdar and Kadane (2012) and Yang and Tokdar (2017) treat the regression coefficients as a function of τ , using smooth monotone curves to model

them under a Gaussian process prior. One of the common issues facing the more general modelling approach is that the likelihood is not available in analytic form, leading to the necessity to numerically approximate the likelihood values for each data observation. A closed-form likelihood approach is proposed by Reich and Smith (2013), who extended the location scale model of He (1997) to more flexibly model the quantile process. More recently, Fang et al. (2015) proposed to use a linearly interpolated approximate likelihood derived from the quantiles, where the pseudo-likelihood is available in analytical form, which approaches the true likelihood with increasing number of quantiles.

In this paper, we make the following contributions. First, we extend and modify the quantile pyramids described in Hjort and Walker (2009) to the regression setting, and we construct a flexible linear quantile model. Second, we show how meaningful priors can be placed directly on the quantiles, which can lead to better estimates. Third, we prove posterior consistency for the conditional quantiles. Finally, we provide an efficient method for parameter estimation via MCMC.

The article is organised as follows. In Section 2 we recall the basic construction of the quantile pyramids studied in Hjort and Walker (2009). The proposed pyramid quantile regression (PQR) modelling is detailed in Section 3, including its theoretical properties and an estimation procedure. Extensive simulation studies are carried out in Section 4,

where the proposed method is compared to the best alternative approaches. In Section 5, real examples illustrate PQR application to extreme quantile modelling and censored data analysis with a large number of covariates. The final section presents concluding discussions.

2 Quantile pyramids for random distributions

Quantile pyramids was introduced by Hjort and Walker (2009) as a method to define a random probability measure for nonparametric Bayesian inference. Contrary to the better known Pólya trees (Ferguson 1974, Lavine 1992, Lavine 1994) that consider random probability masses and fixed partitions, Hjort and Walker (2009) propose the use of random quantiles with fixed probabilities.

The pyramid quantile process that defines a random probability measure on $[0, 1]$ is constructed as follows. Let $Q(\tau)$ be the associated random quantile function, with $Q(0) = 0$ and $Q(1) = 1$. At level $m = 1$ of the construction the median $Q(1/2)$ is randomly generated over $(0, 1)$ according to a given distribution. At level $m = 2$ of the construction the quartile $Q(1/4)$ is sampled on the interval $(0, Q(1/2))$ and $Q(3/4)$ is sampled over $(Q(1/2), 1)$. The process is continued at the following levels m , where the quantiles $Q(j/2^m), j = 1, 3, \dots, 2^m - 1$, are generated conditionally on the quantiles previously sampled. Figure 1(a) demonstrates one sample drawn from this quantile pyramid process for

$m = 1, 2, 3$, where the value of $Q(j/2^m)$ is indicated on the x -axis, and Figure 1(b) shows the intervals from which successive quantiles at different levels were sampled.

Specifically, quantiles at level m are generated after those at level $m - 1$ according to

$$Q(j/2^m) = Q((j-1)/2^m)(1 - V_{mj}) + Q((j+1)/2^m)V_{mj}, \quad (2)$$

where $Q(j/2^m)$ is the new quantile defined at level m and where $Q((j-1)/2^m)$ and $Q((j+1)/2^m)$ are its closest ancestors. The independent variable at work at each level m , V_{mj} , is a random variable on the unit interval. A natural choice is to use V_{mj} 's that are Beta distributed, see Hjort and Walker (2009) for other possibilities. As m tends to infinity the random quantile $Q(\tau)$ is defined for all τ in $(0, 1)$. Notably, the behaviour of this quantile pyramid process depends on these variables. For instance, if at each level we impose that $\mathbb{E}(V_{mj}) = 0.5$, then we have $\mathbb{E}(Q(\tau)) = \tau$ for all τ in $(0, 1)$ and the quantile process is centred at the uniform quantile function. Theoretical results that concern $Q(\tau)$ can be found in Hjort and Walker (2009). They describe for example relatively mild conditions involving decreasing variances of V_{mj} for growing m that ensure *a.s.* the existence of an absolutely continuous $Q(\tau)$.

In practice, to allow a Bayesian inference on the random distribution, the process is stopped at a finite level M and a linear interpolation on the set of quantiles $Q(j/2^M)$,

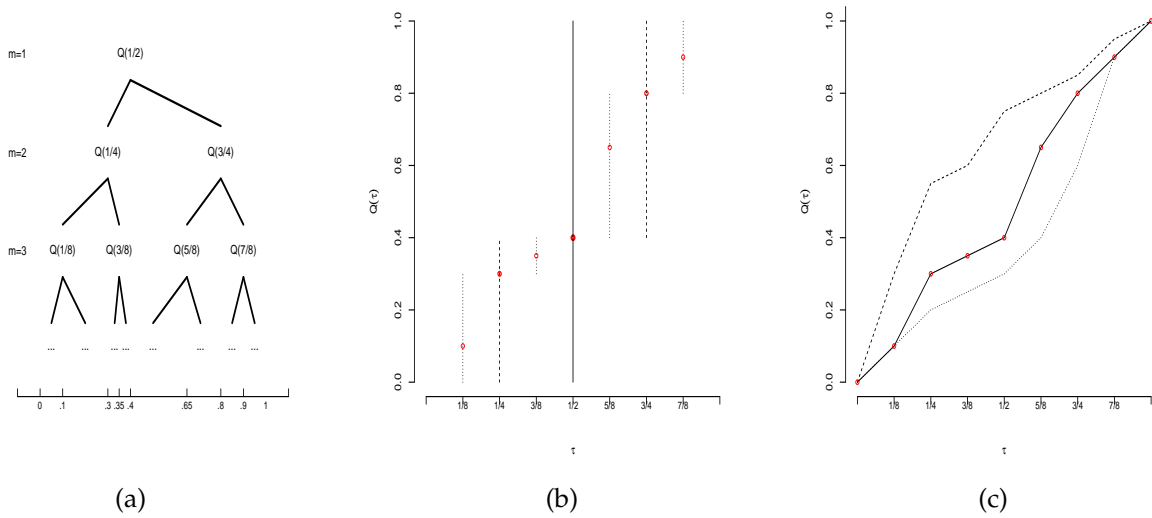


Figure 1: The quantile pyramid generating process. Figure (a) shows the binary tree for one sample drawn from this quantile pyramid process, x -axis indicates the value of $Q(j/2^m)$. In figure (b), the lines indicate the intervals from which the quantile values were sampled. Figure (c) shows the interpolated quantile function, the different curves correspond to different samples of the quantile function.

$j = 0, 1, \dots, 2^M$, completes the process. Figure 1(c) demonstrates three random samples of the piecewise linear quantile functions obtained from the described procedure. The density function corresponding to this linearly interpolated quantile function is piecewise constant, so there is a well defined likelihood function for this random type histogram model. Due to the tree nature of the quantile process, the simultaneous density of the $2^M - 1$ quantiles can be written as

$$\begin{aligned} & \pi \left(Q \left(\frac{1}{2} \right), Q \left(\frac{1}{4} \right), Q \left(\frac{3}{4} \right), \dots, Q \left(\frac{2^{M-1}}{2^M} \right) \right) \\ &= \prod_{m=1}^M \left\{ \prod_{j=1,3,\dots,2^{m-1}} \pi_{mj} \left(Q \left(\frac{j}{2^m} \right) \mid Q \left(\frac{j-1}{2^m} \right), Q \left(\frac{j+1}{2^m} \right) \right) \right\}, \end{aligned} \quad (3)$$

where the densities π_{mj} can be derived from Equation 2, based on the density of V_{mj} ,

through a simple transform of variables.

3 Regression modelling with quantile pyramids

Here we introduce the use of quantile pyramids in the linear regression setting. We consider the general case when several conditional quantiles are of interest, say $Q_\tau(Y|\mathbf{x})$ at quantile levels $\tau = \tau_1, \tau_2, \dots, \tau_T$ with $\tau_1 < \tau_2 < \dots < \tau_T$. The covariate $\mathbf{x} = (x_1, \dots, x_P)$ belongs to a given bounded subset \mathcal{X} of \mathbb{R}^P . In practice \mathcal{X} can be taken as the convex hull of the N observed data points $\mathbf{x}_i, i = 1, \dots, N$.

3.1 Model formulation

The starting point for the model formulation is the simple fact that a hyperplane in \mathbb{R}^{P+1} is determined by the values of $P+1$ of its points. Let $\mathbf{x}^0, \mathbf{x}^1, \dots, \mathbf{x}^P$ denote any $P+1$ locations with corresponding τ th conditional quantile denoted by $Q_\tau^p, p = 0, \dots, P$. Without loss of generality let $\mathbf{x}^0 = (0, \dots, 0), \mathbf{x}^1 = (1, 0, \dots, 0), \mathbf{x}^2 = (0, 1, 0, \dots, 0), \dots, \mathbf{x}^P = (0, \dots, 0, 1)$. The linear quantile regression model for the τ th conditional quantile $Q_Y(\tau|\mathbf{x})$ can be described by the hyperplane passing through these $P + 1$ points

$$\begin{aligned} Q_Y(\tau|\mathbf{x}) &= Q_\tau^0 + \sum_{p=1}^P (Q_\tau^p - Q_\tau^0)x_p \\ &\equiv \beta_0(\tau) + \sum_{p=1}^P \beta_p(\tau)x_p, \end{aligned} \tag{4}$$

where $\beta_0(\tau)$ and $\beta_p(\tau)$ denote the regression coefficients at $\tau = \tau_1, \tau_2, \dots, \tau_T$. For other choices of locations $\mathbf{x}^0, \dots, \mathbf{x}^P$, Equation 4 which is simply the equation of a plane passing through these points has to be modified. In short, the proposed model for simultaneous linear quantile regression uses $P + 1$ independent finite pyramid quantile processes for the quantile functions Q_τ^p . Before proceeding to describe the likelihood, we first present some extensions of these processes that are important in the quantile regression context.

3.2 Oblique quantile pyramid

The quantile pyramid described in Section 2 uses a dyadic partitioning of the probability interval $[0, 1]$. In this setting, the induced quantile levels are all fixed and equally spaced. However, in practice, we may be interested in quantiles at specific levels τ .

In these circumstances, the quantile level of a child node of the pyramid tree is usually no longer located in the middle point of the quantile levels of its closest ancestors. We call this general setting oblique quantile pyramid, as opposed to the regular pyramid previously described. To keep the process centred on the Uniform distribution, we now choose $E(V_{mj})$ to reflect this unequal split using the relative distance from the child quantile level τ_{mj} to its closest ancestors,

$$E(V_{mj}) = \frac{\tau_{mj} - \tau_{mj}^L}{\tau_{mj}^R - \tau_{mj}^L}, \quad (5)$$

where τ_{mj}^L and τ_{mj}^R denote its left and right nearest ancestors' quantile levels, respectively.

From Equations 2 and 5, it is easy to see that $E(Q(\tau)) = \tau$, i.e. under this construction the oblique quantile pyramid is also centred on the Uniform distribution.

The oblique pyramid is constructed via the following procedure. For a sequence of quantiles $Q(\tau_t), t = 1, \dots, T$, the first level of the pyramid at $m = 1$ generates the quantile whose level is halfway into the set of given quantile levels, we will call it the middle quantile level (not to be confounded with the classic median quantile). If T is odd, this is $Q(\tau_{[T/2]+1})$, and given that $V_{11} \sim \text{Beta}(\alpha_{11}, \beta_{11})$, we set α_{11}, β_{11} such that $E(V_{11}) = \tau_{[T/2]+1}$, as $\tau_{11}^L = 0$ and $\tau_{11}^R = 1$ per construction. For the next level $m = 2$, we proceed by getting the middle quantile levels from the left and right of $Q(\tau_{[T/2]+1})$ to be the next nodes, and choose the corresponding $\alpha's, \beta's$ to satisfy Equation 5. The process is then continued until all quantiles in the sequence $Q(\tau_t), t = 1, \dots, T$, have been specified. For identification purposes, if we have an even number of quantile levels, we define the middle value to be the smallest of the two middle quantile levels.

In addition, we choose to have the parameters α_{mj}, β_{mj} increasing with the pyramid level m , which reduces the prior variance for growing m . Throughout this paper, we choose $\alpha_{mj} = 2m$ and $\beta_{mj} = \alpha_{mj} * (1 - E(V_{mj})/E(V_{mj}))$, if $E(V_{mj}) < 0.5$, where $E(V_{mj})$ is calculated using Equation 5. Otherwise, considering the symmetric nature of the Beta

distribution, if $E(V_{mj}) \geq 0.5$, we take $\beta_{mj} = 2m$ and $\alpha_{mj} = \beta_{mj} * E(V_{mj}) / (1 - E(V_{mj}))$. From our experience, this prior is not very informative and gives a good mixing in Markov chain Monte Carlo (MCMC) posterior simulations.

3.3 Centring the prior

Using random quantile functions $Q_\tau^p, p = 0, 1, \dots, P$, for the linear model in Equation 4 defines a prior over the quantile planes. This prior should reflect the prior knowledge with respect to the response Y . The pyramid quantile building process described in Section 3.2 is centred on the Uniform distribution on $[0, 1]$. Let $Q_\tau^{p,unif}, p = 0, 1, \dots, P$, be $P+1$ independent replications of this process. In order to use the pyramid quantiles in Equation 4, for data Y arising from the reals, we can centre each Q_τ^p process on the quantile function of a Normal distribution $\mathcal{N}(\mu^p, (\sigma^p)^2), p = 0, \dots, P$, via a simple transformation suggested in Hjort and Walker (2009),

$$Q_\tau^p = \mu^p + \sigma^p \Phi^{-1}(Q_\tau^{p,unif}), \quad (6)$$

where Φ^{-1} denotes the quantile function of the standard normal distribution, for some mean parameters μ^p and standard deviation parameters σ^p . In this case, for each τ in $(0, 1)$, the median of the random quantile Q_τ^p is the τ th quantile of a Normal distribution $\mathcal{N}(\mu^p, (\sigma^p)^2)$. More generally one can centre the prior on different distributions other than

the Normal, depending on the specific prior knowledge available for the particular application at hand, by setting $Q_\tau^p = Q_{null}(Q_\tau^{p,unif})$ for some arbitrary quantile function Q_{null} . Centring the prior on appropriate distributions can be particularly useful for estimating extreme quantiles, as data is scarce at the tails and the pyramid prior is more informative in the tails. However, it is our experience that, for non-extreme quantiles, results are not very sensitive to the default choice of the Normal distribution. For the clarity of exposition, we use a prior of the form of Equation 6 for the pivotal quantile pyramids $Q_\tau^p, p = 0, \dots, P$, to describe our methodology.

In the finite quantile pyramid context a random density for Q_τ^p can be derived, which is piecewise scaled Normal distribution between the quantiles $Q_{\tau_1}^p, \dots, Q_{\tau_T}^p$. This density is obtained by using a simple change of variable on the piecewise constant density function corresponding to $Q_\tau^{p,unif}$. Figure 2 illustrates some samples of this quantile process, highlighting the piecewise Normal density feature. The examples were simulated from a pyramid process centred on the standard Normal distribution, with $M = 3$, $\tau = 0.125, 0.25, \dots, 0.875$ and $V_{mj} \sim \text{Beta}(a, a)$, for $a = 1$ and 10.

3.4 Likelihood and posterior

Equation 4 gives the desired quantiles of the conditional distribution of Y given $X = \mathbf{x}$, with cdf $F(y|\mathbf{x})$. When priors of the form 6 are used, we need to define the likelihood

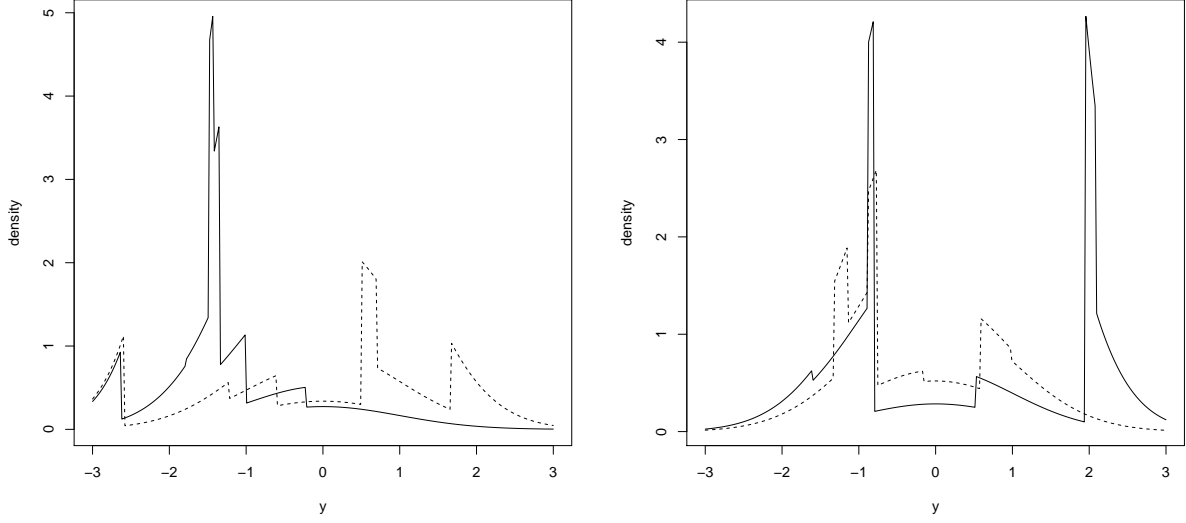


Figure 2: Examples of simulated densities from a finite pyramid process centred on the standard Normal distribution, with $M = 3$ ($\tau = 0.125, 0.25, \dots, 0.875$) and $V_{mj} \sim \text{Beta}(a, a)$, for $a = 1$ (left) and $a = 10$ (right).

function. The chosen option here is to consider that the density $f(y|\mathbf{x})$ of the conditional distribution is piecewise Normal

$$f(y|\mathbf{x}) = \sum_{t=1}^T (\tau_t - \tau_{t-1}) \frac{\phi(y; \mu_{\mathbf{x}}, \sigma_{\mathbf{x}}^2)}{\Phi\left(\frac{Q_Y(\tau_t|\mathbf{x}) - \mu_{\mathbf{x}}}{\sigma_{\mathbf{x}}}\right) - \Phi\left(\frac{Q_Y(\tau_{t-1}|\mathbf{x}) - \mu_{\mathbf{x}}}{\sigma_{\mathbf{x}}}\right)} I_{(Q_Y(\tau_{t-1}|\mathbf{x}), Q_Y(\tau_t|\mathbf{x}))}(y), \quad (7)$$

where $I_{(q_1, q_2]}(y)$ is 1 if $y \in (q_1, q_2]$ and zero otherwise, where $\phi(\cdot; \mu, \sigma^2)$ denotes the density function of a Normal distribution $\mathcal{N}(\mu, \sigma^2)$ and where the parameters $\mu_{\mathbf{x}}$ and $\sigma_{\mathbf{x}}$ change linearly in \mathbf{x}

$$\mu_{\mathbf{x}} = \left(1 - \sum_{p=1}^P x_p\right) \mu^0 + \sum_{p=1}^P x_p \mu^p, \quad \sigma_{\mathbf{x}} = \left(1 - \sum_{p=1}^P x_p\right) \sigma^0 + \sum_{p=1}^P x_p \sigma^p. \quad (8)$$

This formulation implies that the priors on all conditional distributions are centred on the Normal distribution and Equation 8 specifies that the quantiles of these centring distributions change linearly in the covariates. This additional assumption on the form of the prior is quite natural in the linear quantile setting and not overly restrictive. Equation 7 can be obtained by extending the random histogram-type likelihood corresponding to the finite quantile pyramid centred on the uniform distribution as in Hjort and Walker (2009) and applying the relevant transformation of the Equation 6.

Note that a more general approach which does not require the assumption of Equation 8, is to specify the likelihood function by working directly with the density of the conditional distribution $f(y|\mathbf{x}) = \frac{1}{q_{\mathbf{x}}(F(y_i|\mathbf{x}))}$ where $q_{\mathbf{x}}$ denotes the quantile density at \mathbf{x} , *i.e.* the derivative of $Q_Y(\tau|\mathbf{x})$ with respect to τ . Nevertheless, numerical search over a fine grid is required for the evaluation of the density at each data observation, which increases both the numerical error and computational burden. We therefore choose to work with Equation 8 in this article.

The posterior distribution for the finite number of quantile levels τ_1, \dots, τ_T can be obtained for the quantiles $\mathbf{Q}^p = \{Q_{\tau_1}^p, \dots, Q_{\tau_T}^p\}$, $p = 0, \dots, P$, and the associated parameters

$\boldsymbol{\mu} = \{\mu^0, \dots, \mu^P\}$, $\boldsymbol{\sigma} = \{\sigma^0, \dots, \sigma^P\}$, via the usual Bayes theorem

$$\pi(\mathbf{Q}^0, \dots, \mathbf{Q}^P, \boldsymbol{\mu}, \boldsymbol{\sigma} | y_1, \dots, y_N) \propto \prod_{i=1}^N f(y_i | \mathbf{x}_i) \times \prod_{p=0}^P \pi(\mathbf{Q}^p | \mu^p, \sigma^p) \times \pi(\boldsymbol{\mu}) \times \pi(\boldsymbol{\sigma}), \quad (9)$$

where $f(y_i | \mathbf{x}_i)$ is given in Equation 7. The distributions $\pi(\boldsymbol{\mu})$ and $\pi(\boldsymbol{\sigma})$ are hyperpriors for the parameters of the Normal distributions. Throughout the paper these hyperpriors are set to $N(0, 20)$ and $\text{Gamma}(0.001, 0.001)$, for μ^p and σ^p respectively. In addition, using Equations 3 and 6, the pivotal pyramid prior distributions $\pi(\mathbf{Q}^p | \mu^p, \sigma^p)$, $p = 0, \dots, P$, are

$$\begin{aligned} \pi(\mathbf{Q}^p | \mu^p, \sigma^p) &= \prod_{m,j} \pi_{m,j} \left(Q_{\tau_{m,j}}^p | Q_{\tau_{m,j}^L}^p, Q_{\tau_{m,j}^R}^p \right) \\ &= \prod_{m,j} \left\{ g \left(\frac{\Phi \left(\frac{Q_{\tau_{m,j}}^p - \mu^p}{\sigma^p} \right) - \Phi \left(\frac{Q_{\tau_{m,j}^L}^p - \mu^p}{\sigma^p} \right)}{\Phi \left(\frac{Q_{\tau_{m,j}^R}^p - \mu^p}{\sigma^p} \right) - \Phi \left(\frac{Q_{\tau_{m,j}^L}^p - \mu^p}{\sigma^p} \right)} \right) \times \frac{\phi \left(\frac{Q_{\tau_{m,j}}^p - \mu^p}{\sigma^p} \right)}{\Phi \left(\frac{Q_{\tau_{m,j}^R}^p - \mu^p}{\sigma^p} \right) - \Phi \left(\frac{Q_{\tau_{m,j}^L}^p - \mu^p}{\sigma^p} \right)} \right\}, \end{aligned}$$

where $g(\cdot)$ denotes the density of the $V_{m,j}$ variables, throughout the paper $V_{m,j} \sim \text{Beta}(\alpha_{m,j}, \beta_{m,j})$, and ϕ the standard Normal density.

3.5 Non-crossing constraints

The linear model proposed in this paper ensures that the simultaneously fitted quantile planes in Equation 4 do not cross on the convex hull of the $P + 1$ pivotal locations $\mathbf{x}^0, \mathbf{x}^1, \dots, \mathbf{x}^P$. For the single covariate problem, choosing pivotal locations \mathbf{x}^0 and \mathbf{x}^1 to be the minimum and maximum value of \mathcal{X} is sufficient to ensure non-crossing. However,

for $P > 1$, some caution is needed with crossings. If \mathcal{X} corresponds to the convex hull of the observed data points and the pivotal quantiles are placed at $P + 1$ well separated vertices, the non-crossing of the planes needs to be verified at any remaining vertices of the convex hull, say at some points denoted \mathbf{x}^e 's. Note that working with any convex sets larger than the minimum convex set enclosing the data will also ensure non-crossing, but convex sets that are too large puts unnecessary constraints on the regression model, forcing the regression planes to be parallel.

A naive option to ensure non-crossing is to check for crossing at the non-pivotal locations of the convex hull and discard the samples that produce crossing planes during the Metropolis-Hastings MCMC sampling procedure. However, for moderate numbers of covariates, this approach is very inefficient as the crossing will most likely be frequent. In fact, a better solution is to adjust the MCMC proposal distribution so that it proposes only in the non-crossing region. To accomplish that, we will adopt Uniform proposals $U(l_\tau^p, u_\tau^p)$ for Q_τ^p , and choose the lower and upper bounds (l_τ^p, u_τ^p) while ensuring that the corresponding quantiles at the non-pivotal locations do not cross, Fang et al. (2015) used a similar approach working with the entire dataset.

More specifically, for each extra location \mathbf{x}^e on the vertices of the convex hull, the bounds can be easily found by solving $Q_\tau^e = Q_{\tau-1}^e$ and $Q_\tau^e = Q_{\tau+1}^e$ for Q_τ^p based on the

hyperplane equation. For example, for the hyperplane described in Equation 4, when the p th component of \mathbf{x}^e is greater than zero, i.e. $x_p^e > 0$, we have

$$l_\tau^p | \mathbf{x}^e = Q_\tau^0 + \left(Q_{\tau-1}^e - Q_\tau^0 - \sum_{j \neq p} (Q_\tau^j - Q_\tau^0) x_j^e \right) / x_p^e ,$$

$$u_\tau^p | \mathbf{x}^e = Q_\tau^0 + \left(Q_{\tau+1}^e - Q_\tau^0 - \sum_{j \neq p} (Q_\tau^j - Q_\tau^0) x_j^e \right) / x_p^e ,$$

where $l_\tau^p | \mathbf{x}^e$ and $u_\tau^p | \mathbf{x}^e$ are Q_τ^p lower and upper bounds, respectively, based on the crossing restrictions at \mathbf{x}^e . Similarly, if $x_p^e < 0$, the above lower bound becomes the upper bound and vice-versa. Therefore, to take into account all non-pivotal vertices' constraints, we choose $l_\tau^p = \max\{l_\tau^p | \mathbf{x}^e\}$ and $u_\tau^p = \min\{u_\tau^p | \mathbf{x}^e\}$. In this way, non-crossing issues are easily handled. Note that the bounds for each extra location can be found at once through simple matrix operations, not being computationally very expensive.

3.6 Large pyramidal support and posterior consistency

In this section we first study the support of the proposed prior on the quantile planes provided by infinite quantile pyramids. We then give a posterior consistency property of the procedure that uses finite quantile pyramids defined upon a level M_n that grows slowly with the sample size n .

For a formal treatment of these topics in the regression context we follow Yang and

Tokdar (2017) and consider a stochastic design setting where the covariates X_i 's are drawn from a pdf f_X . In order to ensure that the linear model (4) is valid we suppose here that the support \mathcal{X} of f_X is a subset of the convex hull of the pyramid locations $\mathbf{x}^0, \dots, \mathbf{x}^P$. By using infinite quantile pyramids $Q_\tau^0, \dots, Q_\tau^P$, we define a prior probability measure Π on the set $\mathcal{F} = \{f(x, y) = f_X(x)f_Y(y|x)\}$ of density functions on $\mathcal{X} \times \mathbb{R}$.

Let $f^*(x, y) = f_X(x)f_Y^*(y|x)$ be a given density functions on $\mathcal{X} \times \mathbb{R}$, that later will be considered as the true data generating process. Let $d_{KL}(f^*, f) = \int f^* \ln(f^*/f)$ denotes the KL divergence between f^* and f . By extending Proposition 3.1 in Hjort and Walker (2009) to the regression setting we first show that, under some regularity conditions, f^* is in the Kullback-Leibler (KL) support of Π , *i.e.* for any $\epsilon > 0$ we have $\Pi(\{f : d_{KL}(f^*, f) < \epsilon\}) > 0$.

To do this, if for $p = 1, \dots, P$ we take $Q_\tau^p = Q_{null}^p(Q_\tau^{p,unif})$, we first suppose that the conditions ensuring that the processes $Q_\tau^{p,unif}$ are a.s. absolutely continuous are verified, and let $q_p^{unif}(\cdot)$ be the corresponding quantile density function. For each $p = 1, \dots, P$, let also $q_p^*(\cdot)$ be the quantile density function corresponding to the density $f_Y^*(y|\mathbf{x}^p)$ and let $q_p^{*unif}(\cdot)$ be the quantile density function corresponding to the quantile function $Q_p^{*unif}(\cdot) = F_{null}^p(Q_p^*(\cdot))$. The regularity conditions are simply the conditions (A)-(C) described in Hjort and Walker (2009) applied at each pyramid location $\mathbf{x}^0, \dots, \mathbf{x}^P$ plus a regularity condition

on the centring quantile functions Q_{null}^p . More precisely we consider the following conditions

(A) for any $\epsilon > 0$ and for all $p = 1, \dots, P$ we have $\Pi(\{q_p^{unif} : \int q_p^{unif} \ln(q_p^{unif}/q_p^{*unif}) < \epsilon\}) > 0$,

(B) for all $\delta > 0$ and for all $p = 1, \dots, P$ there exists an $\epsilon > 0$ such that

$$\int \ln \frac{q_p^*(\tau_\epsilon(u))}{q_p^*(u)} du < \delta$$

for any function $\tau_\epsilon(u)$ with values in $(0, 1)$ for which $\max_u |\tau_\epsilon(u) - u| < \epsilon$,

(C) for each $p = 1, \dots, P$ the density $f_Y^*(y|\mathbf{x}^p)$ is bounded by a finite value,

(D) for each $p = 1, \dots, P$ the quantile function Q_{null}^p is absolutely continuous.

Proposition 1. *Under the conditions (A)-(D) the density f^* is in the KL support of Π .*

The proof is given in the Appendix. The smoothness condition (B) and the condition of boundary (C) concern only the density f^* . Concerning (A), Hjort and Walker (2009) have shown that this condition is verified by a quantile pyramid Q_τ^{unif} on $[0, 1]$ when the V_{mj} 's have expectations fixed at 0.5 and variances decreasing sufficiently fast, more precisely $\sum_{m=1}^{+\infty} \max_j Var(V_{jm}) < +\infty$. The condition (D) is fulfilled by any quantile function that admits a derivative and corresponds to a distribution with a bounded support. This is

not verified for example in the case when the centring distribution is Gaussian but, in practice, one can consider instead a truncated version on an arbitrarily large interval.

In practice we use finite quantile pyramids defined until a finite level M . A common practice is to use a level M that is size dependent, say M_n , increasing with n . In this case, again by extending a result from Hjort and Walker (2009), we can establish a strong consistency property, called Hellinger consistency, of the resulting prior Π_{M_n} . Let $f^*(x, y) = f^X(x)f_x^*(y)$ be a density in the KL support of Π , the prior constructed with infinite pyramid quantile processes and let (X_i, Y_i) , $i = 1, \dots, n, \dots$ be independent observations from f^* . The Hellinger distance $d_H(f^*, f)$ between the densities f^* and f is defined as $d_H^2(f^*, f) = \int (\sqrt{f^*} - \sqrt{f})^2$. The sequence of posterior distributions $\{\Pi_{M_n}(\cdot | (X_i, Y_i), i = 1, \dots, n)\}_n$ is said to be Hellinger consistent at f^* if, for every $\epsilon > 0$ and for every set

$$A_\epsilon = \{f(x, y) : d_H^2(f^*, f) < \epsilon\}$$

we have $\Pi_{m_n}(A_\epsilon | (X_i, Y_i), i = 1, \dots, n) \rightarrow 1$ a.s.

Proposition 2. *Under the conditions (A)-(C) and if M_n is such that $M_n \rightarrow +\infty$ and $2^{M_n}/n \rightarrow 0$ then the sequence of posterior distributions $\{\Pi_{M_n}(\cdot | (X_i, Y_i), i = 1, \dots, n)\}_n$ is Hellinger consistent at f^* .*

The proof for this proposition is given in the appendix.

4 Simulated examples

In this section, small sample properties of the pyramid quantile regression estimator (PQR) will be investigated through simulation examples. Also, PQR will be compared with three other approaches: semiparametric regression model (BSquare) of Reich and Smith (2013), Gaussian process method (GPQR) of Yang and Tokdar (2017) and the frequentist constrained estimator (freqQR) of Bondell et al. (2010). The comparisons will be undertaken in terms of 95% coverage probabilities and the empirical root mean squared error $RMSE(\tau) = \sqrt{1/s \sum_{s=1}^S [\beta(\tau) - \hat{\beta}_s(\tau)]^2}$, based on $S = 200$ data sets. Following Reich and Smith (2013), we use the simulation designs that are detailed below.

Design 1. $\beta_0(\tau) = \log[\tau/(1 - \tau)], \beta_1(\tau) = 2;$

Design 2. $\beta_0(\tau) = \text{sign}(0.5 - \tau) \log(1 - 2|0.5 - \tau|), \beta_1(\tau) = 2\tau;$

Design 3. $\beta_0(\tau) = \Phi^{-1}(\tau), \beta_1(\tau) = 2 \min\{\tau - 0.5, 0\};$

Design 4. $\beta_0(\tau) = 2\Phi^{-1}(\tau), \beta_1(\tau) = 2 \min\{\tau - 0.5, 0\}, \beta_2(\tau) = 2\tau, \beta_3 = 2, \beta_4 = 1, \beta_5 = 0;$

For each design, we simulated some observations $y_i, i = 1, \dots, N$, from

$$y_i = \beta_0(u_i) + \sum_{j=1}^P x_{ij} \beta_j(u_i),$$

where the j -th covariate is $x_{ij} \stackrel{iid}{\sim} \text{Unif}(-1, 1)$ and $u_i \stackrel{iid}{\sim} \text{Unif}(0, 1)$. The simulated conditional densities at $x = -1$, $f(Y|x = -1)$, for designs 1 to 4 are illustrated in Figure 3.

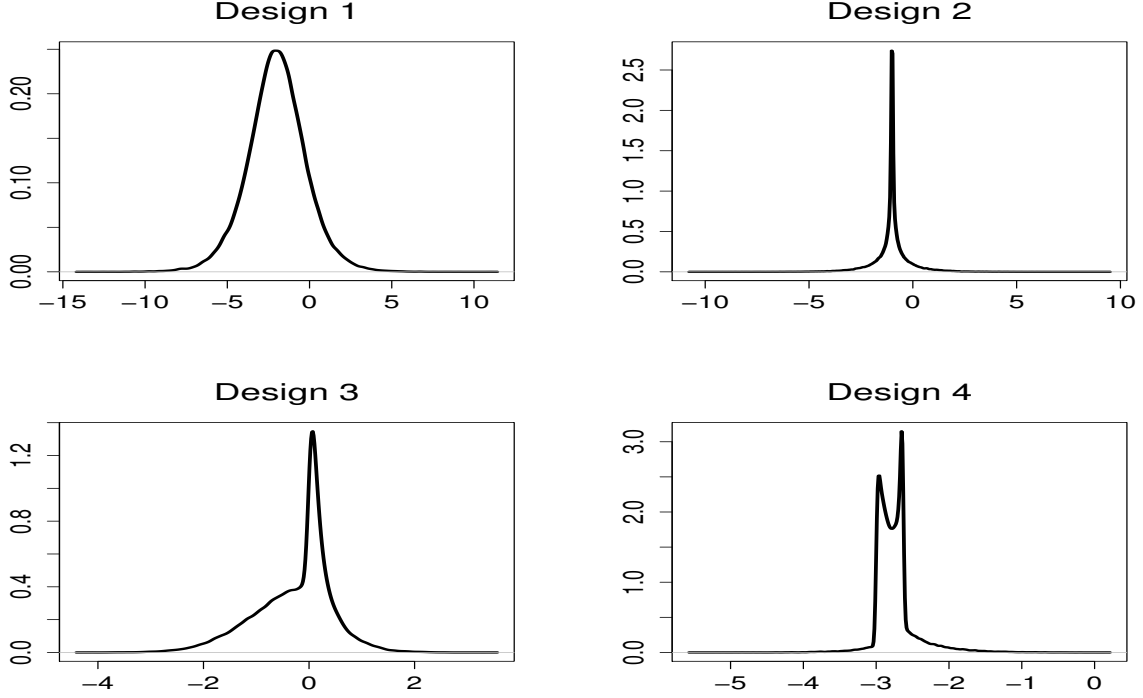


Figure 3: True conditional densities $f(Y|x = -1)$ for the simulation designs.

For univariate designs 1 to 3, we used the datasize $N = 100$ and estimated simultaneously the quantile regression lines at quantile levels $\tau = 0.01, 0.05, 0.10, \dots, 0.95, 0.99$. PQR was fitted based on 110.000 MCMC draws and burn-in of 10.000. Furthermore, in order to improve MCMC mixing, the pyramid quantiles were reparametrised using the logarithm of the difference between adjacent quantile levels, i.e. $\{\log(Q^p(\tau_2) - Q^p(\tau_1)), \dots, \log(Q^p(\tau_T) - Q^p(\tau_{T-1})), \log(Q^p(\tau_1) + Q^p(\tau_T) + c)\}$, where a constant $c = 2|\min(Y_i)|$ was added to the last term to prevent a negative argument in the logarithm function. Poste-

rior means were taken as point estimates for the β 's.

BSquare estimator is implemented in BSquare package (Smith and Reich 2013) in R (R Core Team 2014), to fit this model we used the logistic base distribution with 4 basis functions. GPQR model is also available in R (qrjoint package by Tokdar 2015), and it was estimated from 50.000 MCMC samples, thinning every 10 samples and discarding the initial 20% of the samples as burn-in. Codes for Bondell et al. (2010) are available from first author's web page.

Figure 4 presents RMSE results for the univariate designs. Overall we can see that, for non-extreme quantile levels, all methods perform similarly, with BSquare having the best results for β_1 from Design 1 and PQR having the best results for β_1 from Design 3. Data from design 1 follows BSquare model assumptions, which certainly contributes to its better performance. Design 3 presents a more challenging quantile function, and the flexibility of the proposed approach is an advantage here.

For extreme quantiles, PQR clearly outperforms the other methods for most cases. Once again the flexibility of the proposed approach contributes to this achievement, as well as the reasonable choice of the quantile process centring distribution. Note that, although the simulated designs are not from a Normal distribution (e.g. see Figure 3), yet this is a reasonable centring choice here. The meaningfulness of quantile parameters in

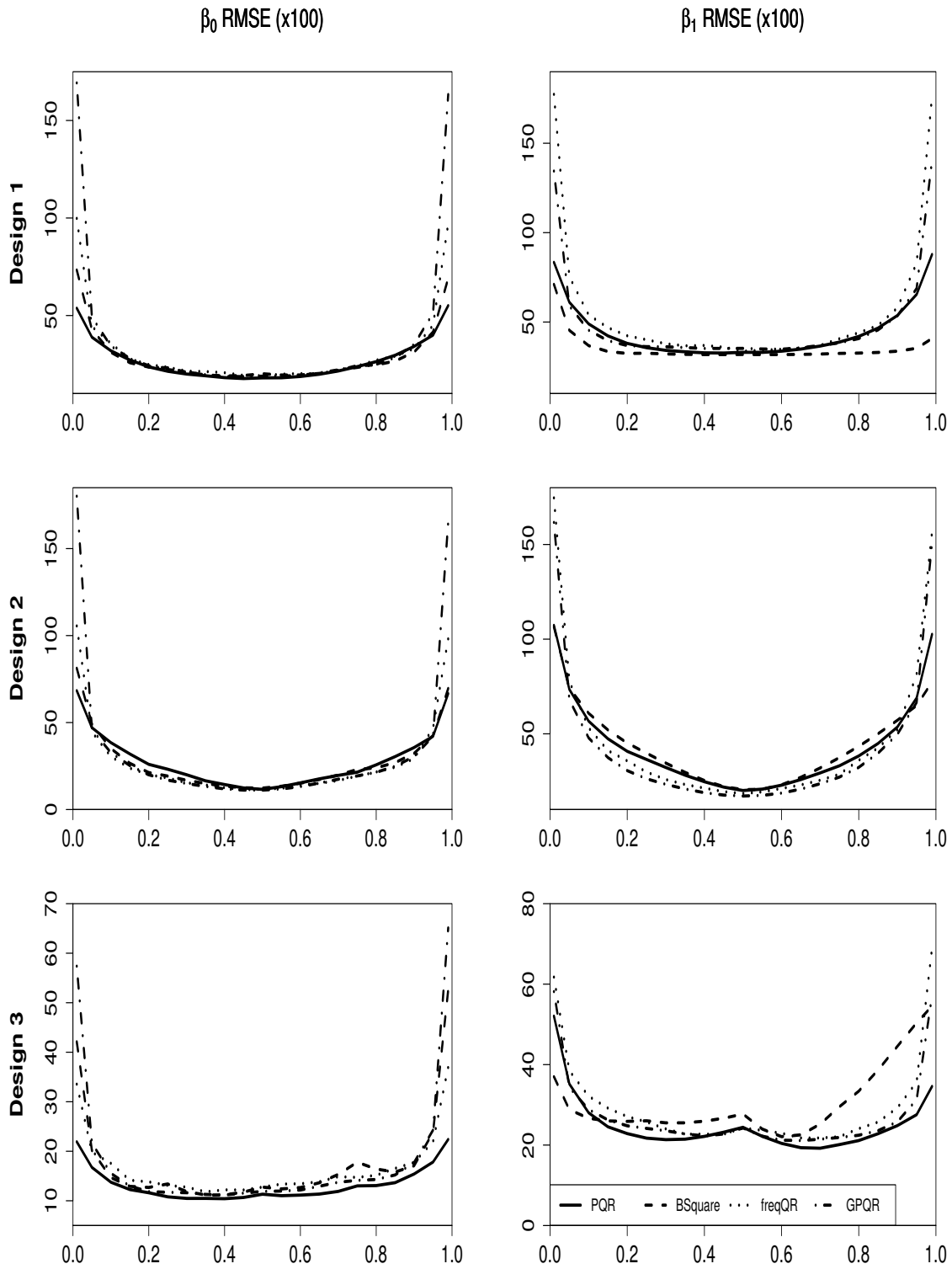


Figure 4: RMSE ($\times 100$) for β_0 (left) and β_1 (right) at $\tau = 0.01, 0.05, 0.1, \dots, 0.95, 0.99$.

PQR is a great feature of the proposed model, as prior information are easily interpreted and incorporated. As shown here, a rough idea of the true distribution can contribute to improve the estimation of extreme quantiles.

Figure 5 shows 95% coverage probabilities at $\tau = 0.01, 0.05, 0.1, \dots, 0.95, 0.99$ for the univariate designs. However, freqQR confidence intervals for the parameters at $\tau = 0.01$ and 0.99 are not available for this sample size, so freqQR results in Figure 5 are truncated at $\tau = 0.05$ and 0.95 , and highlighted by diamond endpoints.

GPQR has poor coverage probabilities for β_0 for extreme quantiles, for which the method also presented high RMSE (Figures 4 and 5). Prior complexity naturally compromises model interpretability and usage, which is a disadvantage of this approach. Prior information might be affecting estimation here, although default settings were used. From Figure 5, we can also see that freqQR coverages are generally too wide for middle quantiles and too narrow at the extremes (for $\tau = 0.05$ and 0.95 , as the more extremes are not available). The BSquare approach performed poorly for some of the parameters. PQR has, in general, nice coverage probabilities compared to the alternative approaches.

For the multivariate design 4, we considered the estimation at quantile levels $\tau = 0.01, 0.05, 0.50$ with $N = 350$ samples. PQR was fitted based on 150.000 MCMC draws and burn-in of 50.000. For the other methods, previous configurations were adopted.

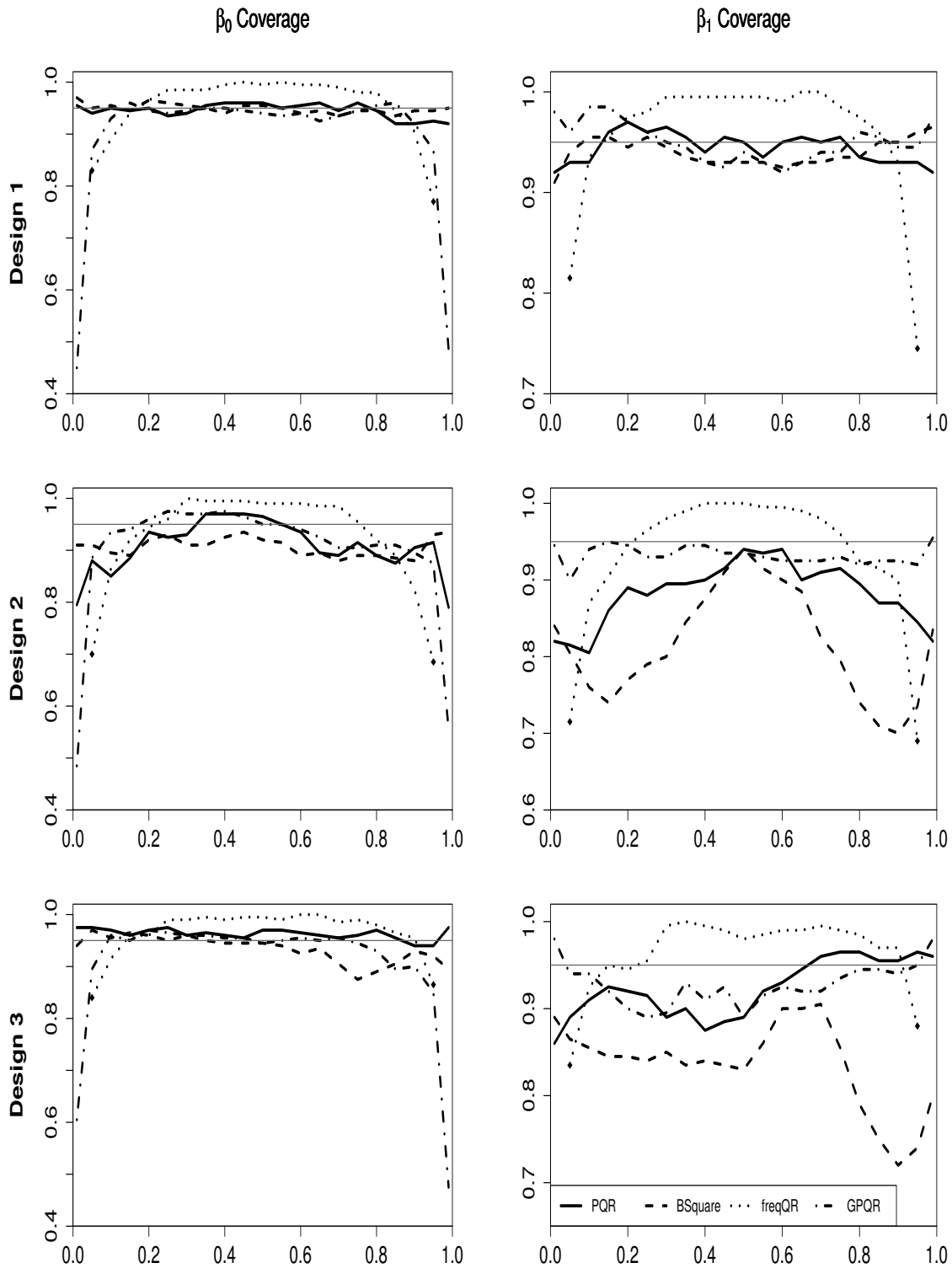


Figure 5: 95% Coverage probabilities for parameters β_0 (left) and β_1 (right) at $\tau = 0.01, 0.05, 0.1, \dots, 0.95, 0.99$. freqQR coverage probabilities at $\tau = 0.01$ and 0.99 are not available, so this curve is truncated at $\tau = 0.05$ and 0.95 (diamond points).

RMSE and coverage results are presented in Tables 1 and 2, respectively.

Table 1: RMSE ($\times 100$) for design 4

	β_0	β_1	β_2	β_3	β_4	β_5
$\tau = 0.50$						
PQR	13.00	24.74	21.15	20.74	20.29	19.19
BSquare	16.13	28.20	26.52	19.85	18.91	19.00
freqQR	13.64	22.37	23.47	21.71	21.14	22.05
GPQR	13.37	24.86	23.00	22.61	21.84	21.03
$\tau = 0.05$						
PQR	21.31	30.61	35.89	32.16	34.63	31.55
BSquare	22.62	65.06	83.90	19.78	19.51	19.32
freqQR	21.86	37.57	39.69	35.90	38.68	37.01
GPQR	20.85	32.44	36.93	32.62	34.58	30.18
$\tau = 0.01$						
PQR	32.73	40.03	48.45	39.74	43.11	38.49
BSquare	65.67	72.44	91.51	19.77	19.50	19.31
freqQR	39.31	52.41	57.09	52.83	54.29	51.39
GPQR	45.67	50.27	57.16	48.12	50.34	46.58

Table 2: 95% Coverage probabilities for design 4

	β_0	β_1	β_2	β_3	β_4	β_5
$\tau = 0.50$						
PQR	0.94	0.90	0.95	0.95	0.96	0.96
BSquare	0.88	0.82	0.90	0.96	0.94	0.94
freqQR	0.98	1.00	0.99	0.98	1.00	0.98
GPQR	0.96	0.86	0.89	0.92	0.95	0.92
$\tau = 0.05$						
PQR	0.96	0.98	0.94	0.98	0.96	0.96
BSquare	0.96	0.19	0.09	0.96	0.94	0.94
freqQR	0.90	0.88	0.86	0.89	0.85	0.90
GPQR	0.92	0.92	0.92	0.96	0.92	0.94
$\tau = 0.01$						
PQR	0.97	0.96	0.91	0.96	0.96	0.98
BSquare	0.72	0.14	0.08	0.96	0.94	0.94
freqQR	0.41	0.52	0.46	0.47	0.48	0.50
GPQR	0.76	0.96	0.97	0.97	0.98	0.97

BSquare had issues in estimating the parameters for this multivariate design. In particular β_0, β_1 and β_2 presented high RMSE's and low coverages, as shown in Tables 1 and 2. In fact, the estimated quantile planes corresponding to different quantile levels were generally parallel, which obviously impacted the estimation of all parameters that vary with τ . This drawback of the non-crossing constraints imposed in Reich and Smith (2013) often happens for multivariate examples, unless large samples are available so that crossing occurs infrequently.

From Table 1, PQR has generally the smallest RMSE, significantly outperforming GPQR at $\tau = 0.01$ and also notably better than freqQR for $\tau = 0.05$ and $\tau = 0.01$. Moreover, among all methods, PQR has coverages closest to the nominal level. As noted before, freqQR has coverages consistently above the nominal level at $\tau = 0.50$ and below it at the extremes ($\tau = 0.05$ and $\tau = 0.01$). Again GPQR has poor coverage for β_0 for extreme quantiles.

Note that PQR has great performance despite the small number of pyramid levels ($M = 2, \tau = 0.01, 0.05, 0.50$). Indeed, increasing M does not significantly affect the results, corroborating the proximity between the least false and true parameter values.

We have restricted our simulation studies to relatively small sample sizes since in large samples, the simple minimization problem proposed by Koenker and Bassett (1978)

has great coverages and generally small errors, as shown in Yang and Tokdar (2017). Under our framework, we would expect MCMC to converge faster since in large samples crossing of quantiles is less likely to occur and hence slow down the MCMC sampling algorithm. In terms of computational cost, around 80% of the computational overhead is attributable to the likelihood calculation. This is mostly due to the indicator function in Equation (7). For example, the times it takes to compute one likelihood using non-optimised codes, for multivariate design 4, are 3×10^{-4} seconds for $N = 350$ and 2×10^{-3} seconds for $N = 3500$, in a 3.6GHz quad-core Intel i7-4790k CPU. However, the likelihood evaluations are highly parallelisable and runtimes can be reduced dramatically. The additional computational burden with increasing number of covariates is insignificant compared to the cost of likelihood evaluations, but of course it causes a linear increase in the number of parameters updated at each iteration, $(P + 1) * (T + 2)$.

5 Real examples

In this section, we illustrate the proposed method on two publicly available real datasets, one involving extremal quantile modelling and a censored data analysis involving a large number of covariates.

5.1 Extreme quantile modelling

In extreme value analysis, it is common practice to use the so-called extreme value distributions to make inference on the tails of the distribution of the data. Using a parametric model places strong assumptions on the data, but is an attractive approach since data is often scarce in the extremal regions. However, a long standing issue is the fidelity of the data to the parametric assumptions, see Coles (2001). We propose in this application to model linear quantiles of extreme data using PQR, that allows us to drop these parametric assumptions, but instead use the information from extreme distributions as prior when centring the quantile process.

Here we will apply PQR to model extreme tropical cyclones. The dataset consists of 82 observations of cyclones whose wind speed is greater than 96 knots (kt) threshold, recorded in the US coast from 1899 to 2006 (this is an updated version of the data analysed in Jagger and Elsner 2009 which included 79 cyclones; the update is available in the authors' webpage). Jagger and Elsner (2009) considers that these data follow a Generalized Pareto Distribution (GPD), with cdf given by

$$G(y) = 1 - [1 + \xi(y - \mu)/\sigma]_+^{-1/\xi},$$

where $(h)_+ = \max(h, 0)$, μ is the fixed threshold, and $\sigma > 0$ and ξ are the scale and shape

parameters respectively.

Therefore, we consider fitting PQR using GPD as the quantile process centring distribution. Similarly to the Gaussian case we assume here that the unknown parameters (σ , ξ) change linearly in x . Furthermore, we use $\text{Gamma}(0.001, 0.001)$ and $U(0, 1000)$ as hyperpriors for σ and ξ , respectively. Following Jagger and Elsner (2009), we model extreme tropical cyclone (TC) wind speed quantiles at $\tau = 0.10, 0.25, 0.50, 0.75, 0.90$ as a function of the Southern Oscillation Index (SOI) and the sunspot number (SSN), both averaged over August-October and standardised. We used for the estimation 60.000 MCMC draws and burn-in of 10.000. Figure 6(b-d) presents the parameter estimates and 90% confidence interval for PQR, obtained as the upper and lower 0.05 sample quantiles of the posterior samples. For comparison, BSquare, freqQR and GPQR estimates are also indicated.

As illustrated in Figure 6, wind speed increases with decreasing SOI, which is expected as small SOI is associated with El Nino warming events, which in turn favour extreme cyclones, as explained in Jagger and Elsner (2009). As in Jagger and Elsner (2009), SSN is generally positive associated with extreme winds, but this is not a statistically significant association. From SOI parameter estimates' plot, we can also see that PQR provides smoother and nicer estimates than freqQR, which lack borrowing strength from the neighbours τ . Due to the rigid non-crossing constraints, BSquare parameter estimates

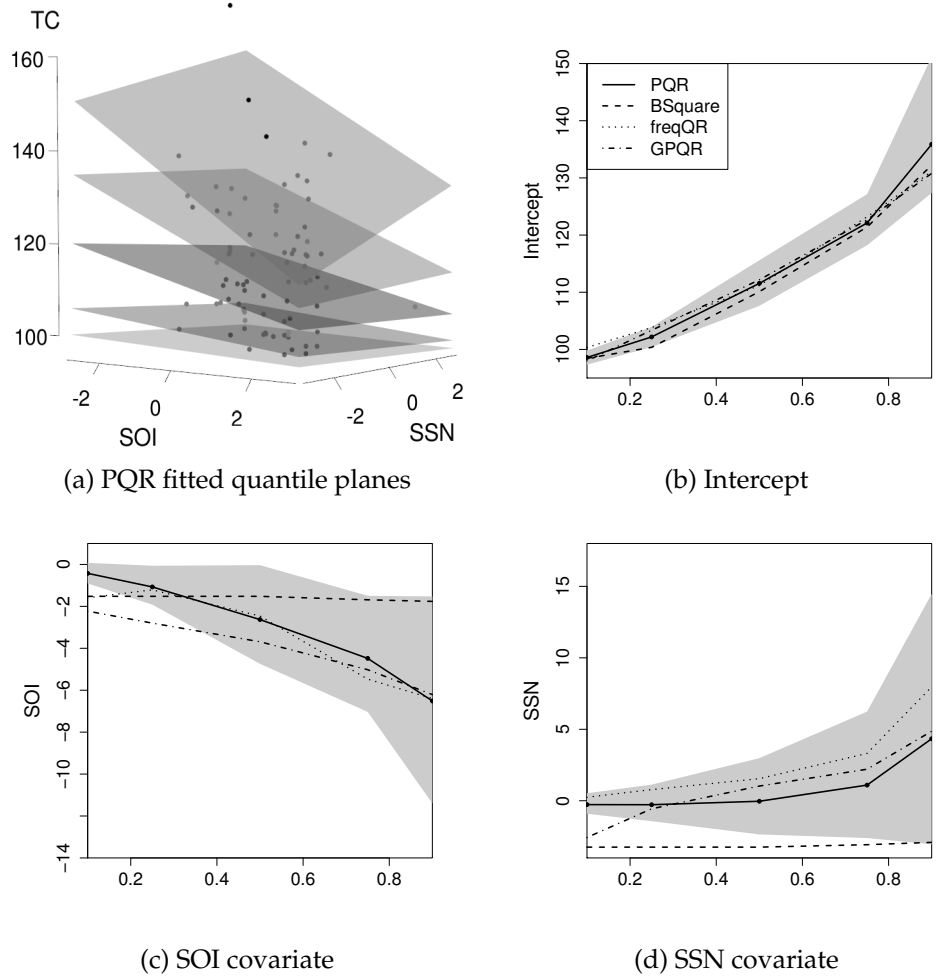


Figure 6: Estimation of extreme tropical cyclone wind speed (TC, in knots) at $\tau = 0.10, 0.25, 0.50, 0.75, 0.90$. (a) PQR fitted quantile planes. (b-d) Parameter estimates using PQR (solid line), BSquare (dashed line), freqQR (dotted line) and GPQR (dash-dotted line). The grey shading indicates 90% confidence interval for PQR.

SOI and SSN are constant and lie mostly outside PQR 90% confidence interval. GPQR produced generally smaller estimates than PQR and freqQR in the SOI parameter across the quantile levels. For the SSN parameter, GPQR produced smaller estimates only in the lower quantiles, while the other estimates largely agree with PQR and freqQR. Therefore, in the event that the data truly follow the GPD distribution, by placing priors centered

on this distribution, we retain some advantages of using the parametric model for inference, and should perform better than models that cannot incorporate this information. However, in the case where data deviates from GPD, the pyramid quantile framework can correct for this misspecification with increasing data. So the ability of the pyramid quantiles to place informative priors allows us to fully take advantage of the Bayesian inferential framework.

5.2 Analysis of censored data

Regression with large numbers of covariates poses additional computational challenges for the proposed method. Here we consider the University of Massachusetts Aids Research Unit IMPACT study data (UIS) available in the `quantreg` package in R, from Hosmer and Lemeshow (1998), and analysed by Portnoy (2003), Reich and Smith (2013) and Yang and Tokdar (2017) using quantile regression. For this analysis with right censoring, the log-likelihood is now the sum over $i = 1, \dots, n$ of

$$(1 - c_i) \log f(y_i | \mathbf{x}_i) + c_i \log(1 - F(y_i | \mathbf{x}_i))$$

where $f(y_i | \mathbf{x}_i)$ is given by Equation 7, where $F(y_i | \mathbf{x}_i)$ is the corresponding CDF and where c_i is the censoring status (1=right censored, 0=otherwise).

The dataset contains records for 575 observations, we estimated the conditional quan-

tiles for the logarithm of the time to return to drug use (Y) as linear functions of 8 predictors, BECK (a depression score), FRAC (a compliance factor), AGE (age at enrollment), TREAT (current treatment assignment, 1= Long course, 0=Short course), NDT (number of previous drug treatment), RACE (1=Non-white, 0=White), IV3 (recent intravenous drug use, 1=Yes, 0=No), SITE (treatment site). All variables were scaled by subtracting their mean and dividing by their range. We fit the quantile levels $\tau = 0.1, 0.2, \dots, 0.9$ using 9 quantile pyramids and the Gaussian centring distribution, this amounts to a problem with 99 parameters. For high dimensions, the strategy described in Section 3.5 requires several modifications.

Firstly, existing off-the-shelf convex hull algorithms encounter memory problems for dimensions higher than 7 or 8. Here our strategy is to compute the convex hull of the data expressed in the space given by their leading 5 or 6 principal components, then to choose the remaining vertices by random sampling. We trial 500 random samples in this fashion, and select the pyramid locations that has the maximum distance between the quantile levels over the $P + 1$ locations. Non-crossing constraint is then verified at all data points.

In higher dimensions, we also have noticed that well placed pyramid locations can greatly improve the MCMC mixing since the parameters are often highly correlated. For the current problem, we perform several parallel runs, each corresponding to a different

set of pyramid locations, and choose the best mixing chain. More precisely for each chain we performed a trial MCMC run of 20.000 of standard MCMC, updating one parameter at a time, with tuning of proposal variance to obtain acceptance probability of roughly 0.44 for each parameter. This step allows us to learn the covariance structure of the parameters.

The next stage of MCMC incorporates the information learned in the first stage, by blocking variables into separate groups at each quantile level (over covariates) and groups at each covariate level (over quantiles), as well as blocking all the centring parameters μ^p in one block and all the variance parameters σ^p in another. At each iteration of the MCMC, all blocks of the quantiles are updated once, followed by the blocks for μ^p and σ^p . The blocks are updated using the learned covariance matrix from the first stage, and a random walk proposal with Gaussian and truncated Gaussian respectively. For each quantile block, we iteratively updated each component parameter within the block, by first updating one parameter independently, using the proposal strategy of Section 3.5, and then updating the following parameters of the block using their conditional distribution and the covariance structure. Again, non-crossing is verified at each data point as we update each parameter. We found that adding this second MCMC run tend to provide more reliable MCMC output that mixes well for most of the pyramid choices. We ran this second stage for 200.000 iterations with 20.000 samples as burn in.

Figure 7 show the estimated coefficients over different quantile levels, PQR estimates are given by solid lines. We also implemented the method of Portnoy (2003) (dotted line) and Yang and Tokdar (2017) (dash dotted line). The method of Portnoy (2003) was used to compute the first eight quantile levels, since it does not produce results for quantile level 0.9 or higher. The three methods produced similar results for the lower quantile levels. For a comparison, we computed the check loss (defined in Section 1) at each of the quantile levels $\tau = 0.1, 0.2, \dots, 0.9$, by summing over $\rho_\tau(y_i - \widehat{Q}_Y(\tau|\mathbf{X}_i))$, where y_i s are the un-censored observations, and \mathbf{X}_i are the corresponding covariate values. The final subplot in Figure 7 shows the computed loss for the three methods. For lower quantiles, there's little difference, whereas the method of Portnoy (2003) is better for moderate to high quantiles, they do not produce estimates for very high quantiles, nor do they ensure non-crossing. PQR out-performs the other two methods in terms of check loss for higher quantiles, see middle figure in the last row of Figure 7. A similar result is seen in the predictive check loss, when we used 10% of the data as test data, see last figure in Figure 7, where the out-of-sample loss is computed as the sum over 10 different sets of randomly selected test data sets, here the improvements in the tails of the distributions are more marked than the in-sample performance.

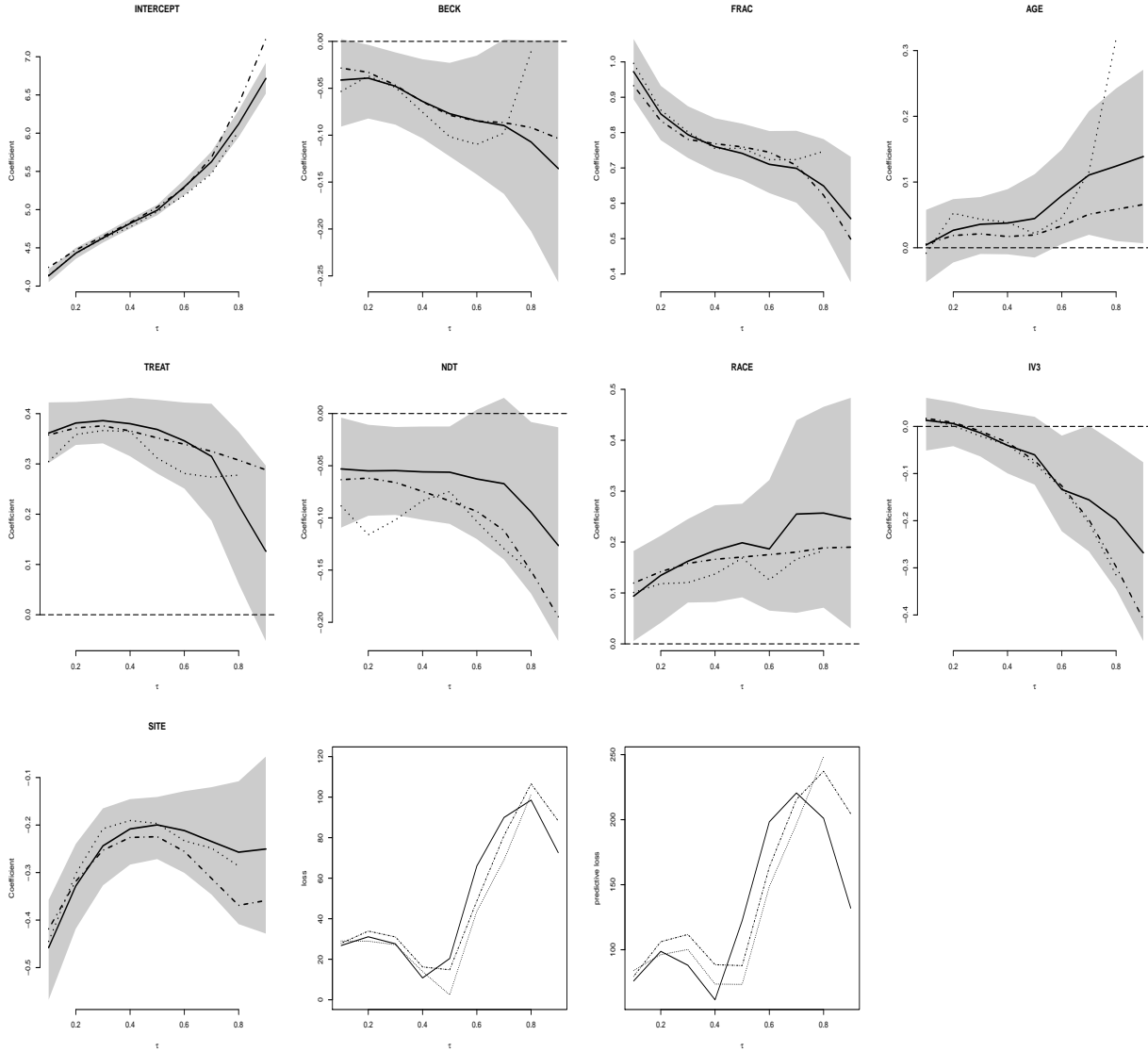


Figure 7: Estimation of regression coefficients for UIS data analysis at $\tau = 0.1, 0.2, \dots, 0.8, 0.9$. Each subplot shows the posterior mean of regression coefficient for the respective covariate using PQR (solid line), freqQR (dotted line) and GPQR (dash-dotted line), dashed line indicates the value at 0. The grey shading indicates 90% confidence interval for PQR. Final plots shows the check loss and predictive check loss.

6 Discussion

This paper proposes a novel simultaneous linear quantile regression model, named pyramid quantile regression (PQR), by using the quantile pyramids prior of Hjort and Walker (2009) as a basis for building a flexible, nonparametric conditional density.

PQR avoids strong parametric assumptions about the conditional distributions, which adds great modelling flexibility and circumvents the need to make parametric assumptions about the distribution of the data. In addition, the model is parametrised in terms of the quantiles themselves, this is a natural way of modelling quantile regression and allows for easy interpretation and incorporation of prior information. For instance, one can centre the conditional quantile priors on chosen distributions based on prior knowledge. We considered centring it on the Normal distribution, and showed that this choice by default works well for a variety of cases, including mildly asymmetric densities. Additionally, PQR can be used for flexible extreme quantile modelling by centring the prior on an extreme distribution, as opposed to strictly requiring the data to follow the parametric assumption, as is often the case in extreme value modelling. We illustrated this application in the modelling of extreme tropical cyclone winds in the US coast using pyramid prior centred on the Generalised Pareto Distribution (GPD). The availability of an explicit expression for a likelihood affords easier extensions to more complex modelling. We have

shown via simulation studies that PQR provides robust estimates with small errors and great coverages properties.

We have demonstrated that the conditional quantiles implied by the linear regression model retains posterior consistency. Our experience with empirical studies also shows that M does not need to be large to obtain reasonable results.

Acknowledgements

TR is funded by CAPES Foundation via the Science Without Borders (BEX 0979/13-9). TR and YF are grateful to the Australian Research Council Centre of Excellence for Mathematical and Statistical Frontiers for support.

References

- Bondell, H. D., B. J. Reich, and H. Wang (2010). Noncrossing quantile regression curve estimation. *Biometrika* 97(4), 825–838.
- Chernozhukov, V., I. Fernandez-Val, and A. Galichon (2009). Improving point and interval estimators of monotone functions by rearrangement. *Biometrika* 96, 559–575.
- Coles, S. G. (2001). *An introduction to statistical modeling of extreme values*. Springer Verlag, London.
- Dette, H. and S. Volgushev (2008). Non-crossing non-parametric estimates of quantile

- curves. *Journal of Royal Statistical Society B* 70, 609–627.
- Fang, Y., Y. Chen, and X. He (2015). Bayesian quantile regression with approximate likelihood. *Bernoulli* 21(2), 832–580.
- Ferguson, T. S. (1974). Prior distributions on spaces of probability measures. *Annals of Statistics* 2, 615–629.
- Hall, P., R. C. L. Wolff, and Q. Yao (1999). Methods for estimating a conditional distribution function. *Journal of American Statistical Association* 94, 154–163.
- Hanson, T. and W. O. Johnson (2002). Modelling regression error with a mixture of Pólya trees. *Journal of American Statistical Association* 97(460), 1020–1033.
- He, X. (1997). Quantile curves without crossing. *American Statistician* 51, 186–192.
- Hjort, N. L. and S. G. Walker (2009). Quantile pyramids for Bayesian nonparametrics. *Annals of Statistics* 37(1), 105–131.
- Hosmer, D. and S. Lemeshow (1998). *Applied survival analysis: Regression modeling of time to event data*. New York: John Wiley and Sons Inc.
- Jagger, T. H. and J. B. Elsner (2009). Modeling tropical cyclone intensity with quantile regression. *International Journal of Climatology* 29, 1351–1361.
- Koenker, R. (2005). *Quantile regression*, Volume 38 of *Econometric Society Monographs*.

Cambridge: Cambridge University Press.

Koenker, R. and J. Bassett, Gilbert (1978). Regression quantiles. *Econometrica* 46(1), 33–50.

Kottas, A. and A. E. Gelfand (2001). Bayesian semiparametric median regression modelling. *Journal of American Statistical Association* 96, 1458–1468.

Kottas, A. and M. Krnjajić (2009). Bayesian semiparametric modelling in quantile regression. *Scandinavian Journal of Statistics* 36, 297–319.

Lavine, M. (1992). Some aspects of Pólya tree distributions for statistical modelling. *Annals of Statistics* 20(3), 1222–1235.

Lavine, M. (1994). More aspects of Pólya tree distributions for statistical modelling. *Annals of Statistics* 22, 1161–1176.

Portnoy, S. (2003). Censored quantile regression. *Journal of American Statistical Association*, 1001–1012.

R Core Team (2014). *R: A Language and Environment for Statistical Computing*. Vienna, Austria: R Foundation for Statistical Computing.

Reich, B. J., H. D. Bondell, and H. J. Wang (2008). Flexible Bayesian quantile regression for independent and clustered data. *Biostatistics* 11, 337–352.

- Reich, B. J., M. Fuentes, and D. B. Dunson (2011). Bayesian spatial quantile regression. *Journal of the American Statistical Association* 106(493), 6–20.
- Reich, B. J. and L. B. Smith (2013). Bayesian quantile regression for censored data. *Biometrics* 69, 651–660.
- Rodrigues, T. and Y. Fan (2016). Regression adjustment for noncrossing Bayesian quantile regression. *Journal of Computational and Graphical Statistics*. (in press).
- Smith, L. and B. Reich (2013). *BSquare: Bayesian Simultaneous Quantile Regression*. R package version 1.1.
- Sriram, K., R. V. Ramamoorthi, and P. Ghosh (2013). Posterior consistency of bayesian quantile regression based on the misspecified asymmetric Laplace density. *Bayesian Analysis* 8(2), 1–26.
- Tokdar, S. (2015). *qrjoint: Joint Estimation in Linear Quantile Regression*. R package version 0.1-1.
- Tokdar, S. T. and J. B. Kadane (2012). Simultaneous linear quantile regression: a semiparametric Bayesian approach. *Bayesian Analysis* 7(1), 51–72.
- Yang, Y. and S. Tokdar (2017). Joint estimation of quantile planes over arbitrary predictor spaces. *Journal of the American Statistical Association*. (in press).

Yu, K. and R. A. Moyeed (2001). Bayesian quantile regression. *Statist. Probab. Lett.* 54(4), 437–447.

Appendix

For clarity we give the demonstrations for the case $P = 1$, the generalization to $P > 1$ with \mathcal{X} within the convex hull of the pyramid locations $\mathbf{x}^0, \dots, \mathbf{x}^P$ being straightforward.

For $P = 1$, without loss of generality, we suppose that $\mathbf{x}^0 = 0$ and $\mathbf{x}^1 = 1$ so that, for $0 < \tau < 1$ and any $0 \leq x \leq 1$,

$$Q_Y(\tau|x) = (1-x)Q_\tau^0 + xQ_\tau^1$$

where Q_τ^0 and Q_τ^1 are independent pyramid quantile processes. We have $Q_\tau^0 = Q_{null}^0(Q_\tau^{0,unif})$ and $Q_\tau^1 = Q_{null}^1(Q_\tau^{1,unif})$ where $Q_\tau^{0,unif}$ and $Q_\tau^{1,unif}$ are independent pyramid quantile processes centered on the uniform distribution on $(0, 1)$. We suppose that $Q_\tau^{0,unif}$ and $Q_\tau^{1,unif}$ are a.s. absolutely continuous and we suppose that the two centring quantile functions Q_{null}^0 and Q_{null}^1 are also absolutely continuous. Thus Q_τ^0 and Q_τ^1 are a.s. absolutely continuous and we denote $q_0(\cdot)$ and $q_1(\cdot)$ the corresponding quantile density functions. Then, for any $0 \leq x \leq 1$, the conditional quantile function $Q_Y(\tau|x)$ is also a.s. absolutely continuous with quantile density function $q_x(u) = (1-x)q_0(u) + xq_1(u)$.

Proof of Proposition 1

We first show that conditions similar to (B) and (C) are also true at any $x \in (0, 1)$:

(B_x) for all $\delta > 0$ there exists an $\epsilon > 0$ such that, $\forall x \in (0, 1)$,

$$\int \ln \frac{q_x^*(\tau_\epsilon(u))}{q_x^*(u)} du < \delta$$

for any function $\tau_\epsilon(u)$ from $[0, 1]$ to $[0, 1]$ for which $\max_u |\tau_\epsilon(u) - u| < \epsilon$.

We use the log sum inequality and see that, $\forall x \in (0, 1)$,

$$\begin{aligned} \int \ln \frac{q_x^*(\tau_\epsilon(u))}{q_x^*(u)} du &= \int \ln \frac{(1-x)q_0^*(\tau_\epsilon(u)) + xq_1^*(\tau_\epsilon(u))}{(1-x)q_0^*(u) + xq_1^*(u)} du \\ &\leq \int \frac{1}{(1-x)q_0^*(\tau_\epsilon(u)) + xq_1^*(\tau_\epsilon(u))} \left\{ (1-x)q_0^*(\tau_\epsilon(u)) \ln \frac{q_0^*(\tau_\epsilon(u))}{q_0^*(u)} \right. \\ &\quad \left. + xq_1^*(\tau_\epsilon(u)) \ln \frac{q_1^*(\tau_\epsilon(u))}{q_1^*(u)} \right\} du \\ &\leq \int \ln \frac{q_0^*(\tau_\epsilon(u))}{q_0^*(u)} du + \int \ln \frac{q_1^*(\tau_\epsilon(u))}{q_1^*(u)} du \end{aligned}$$

and by using condition (B) we get the result.

(C_x) $\forall x \in (0, 1)$ the density f_x is bounded by some $K < \infty$.

Under the condition (C) f_0 and f_1 are bounded by some finite K_0 and K_1 . Since

$f_x(\cdot) = 1/q_x(F_x(\cdot))$ we have, $\forall x \in (0, 1)$,

$$q_x(\cdot) = (1-x)q_0(\cdot) + xq_1(\cdot) > (1-x)\frac{1}{K_0} + x\frac{1}{K_1}$$

thus, $\forall x \in (0, 1)$,

$$f_x(\cdot) < \left\{ (1-x)\frac{1}{K_0} + x\frac{1}{K_1} \right\}^{-1} < \infty.$$

Once these properties are stated we can follow step by step the lines of the proof of Proposition 3.1 in Hjort and Walker (2009). For any x in $(0, 1)$, by using the change of variable $u = F_x^*(y)$, the Kullback-Leibler divergence between f_x^* and f_x can be decomposed as

$$\begin{aligned} \int f_x^*(y) \ln \frac{f_x^*(y)}{f_x(y)} dy &= \int \ln \frac{q_x(\tau_x(u))}{q_x^*(u)} du \\ &= \int \ln \frac{q_x(\tau_x(u))}{q_x^*(\tau_x(u))} du + \int \ln \frac{q_x^*(\tau_x(u))}{q_x^*(u)} du \end{aligned}$$

where $\tau_x(u) = F_x(Q_x^*(u))$. Proceeding as in Hjort and Walker (2009), and using conditions (B_x) and (C_x) , the first term in this sum is smaller than any arbitrary positive value with positive prior probability mass if, for any $\epsilon > 0$, the prior puts positive probability mass on $\{Q_x : \max_u |\lambda_x(u) - u| < \epsilon\}$ where $\lambda_x(u) = F_x^*(Q_x(u))$. To prove that this sufficient condition is true note that we have, $\forall u \in (0, 1)$,

$$\begin{aligned} |Q_x(u) - Q_x^*(u)| &= |(1-x)(Q_\tau^0(u) - Q_\tau^{*0}(u)) + x(Q_\tau^1(u) - Q_\tau^{*1}(u))| \\ &\leq |Q_\tau^0(u) - Q_\tau^{*0}(u)| + |Q_\tau^1(u) - Q_\tau^{*1}(u)|. \end{aligned}$$

Now, from condition (A), the prior puts positive probability mass on $\{Q_\tau^{0,unif} : \max_u |Q_\tau^{0,unif}(u) -$

$Q_\tau^{*0,unif}(u)| < \theta^0\}$ and $\{Q_\tau^{1,unif} : \max_u |Q_\tau^{1,unif}(u) - Q_\tau^{*1,unif}(u)| < \theta^1\}$ for any positive θ^0 and θ^1 . Thus, from the absolute continuity of Q_{null}^0 and Q_{null}^1 , the prior puts positive probability mass on $\{Q_\tau^0 : \max_u |Q_\tau^0(u) - Q_\tau^{*0}(u)| < \delta^0\}$ and $\{Q_\tau^1 : \max_u |Q_\tau^1(u) - Q_\tau^{*1}(u)| < \delta^1\}$ for any positive δ^0 and δ^1 and so, using the preceding inequality, puts positive probability mass on $\{Q_x : \max_u |Q_x(u) - Q_x^*(u)| < \delta\}$ for any positive δ . By using the absolute continuity of F_x^* we finally get that, for any positive ϵ , the prior puts positive probability mass on $\{Q_x : \max_u |\lambda_x(u) - u| < \epsilon\}$.

For the second term in the sum we use again the consequence of condition (A): the prior puts positive probability mass on $\{Q_x : \max_u |Q_x(u) - Q_x^*(u)| < \delta\}$ for any positive δ then, using the absolute continuity of F_x , puts positive probability mass on $\{F_x : \max_u |\tau_x(u) - u| < \epsilon\}$ for any $\epsilon > 0$. Hence, using the property (B_x) , this term is also bounded by any positive real with positive probability and finally we know that the prior put positive probability mass on $\{f_x : d_{KL}(f_x^*, f_x) < \epsilon\}$.

To complete the proof note that this result is true for any $x \in (0, 1)$ and we have, for any $\epsilon > 0$,

$$\Pi(\{f : \forall 0 \leq x \leq 1 d_{KL}(f_x^*, f_x) < \epsilon\}) > 0.$$

Since

$$d_{KL}(f^*, f) = \int d_{KL}(f_x^*, f_x) f_X(x) dx$$

we get the desired result. \square

Proof of Proposition 2

We have just to follow the steps of the proof of proposition 7.1 in Hjort and Walker (2009)

and to note that the Hellinger distance is given by

$$d_h^2(f^*, f) = \int d_H(f_x^*, f_x) f_X(x) dx$$

and that, if q_{kj} , $j = 1, \dots, 2^{M_n} - 1$, $k = 0, 1$ are the quantile sampled by Π_{M_n} , if for $j = 1, \dots, 2^{M_n} - 1$, if we have both $|q_{0j} - q_{0j}^*| < \epsilon$ and $|q_{1j} - q_{1j}^*| < \epsilon$ then, $\forall x \in (0, 1)$,

$$|q_{xj} - q_{xj}^*| \leq (1 - x)|q_{0j} - q_{0j}^*| + x|q_{1j} - q_{1j}^*| \leq \epsilon.$$

It turns out that, for a given $\delta > 0$, $\forall x \in (0, 1)$, there exists $\epsilon > 0$ such that if $|q_{0j} - q_{0j}^*| < \epsilon$

and $|q_{1j} - q_{1j}^*| < \epsilon$ then $d_H^2(f^*, f) < \delta$. Once this is stated the rest of the proof of Hjort and

Walker (2009) applies. \square